Particle ID performance of Liquid Argon TPC

J-PARC T32 collaboration

Abstract

This paper describes a study of particle identification performance of liquid Argon TPC (LArTPC) detector using well-defined charged particles (pions, kaons, and protons) with momentum of 800 MeV/c obtained at J-PARC K1.1Br beamline.

We have build a LArTPC detector with fiducial mass of 150 kg, and injected the beam particle

Keywords:

1. Introduction

Refer [1] for hardware/beam line description

2. Data Quality

2.1. Collected Data

Table 2 shows list of the collected data while Oct/2010 Run. 800 MeV/c pion is expected to pass-through the detector as MIP, and have uniform energy deposition to all the TPC channels. So this data set is very useful for calibrating the detector response (See section xxx). 800 MeV/c proton stops after 15 cm of flight distance inside the TPC fiducial volume with relatively large dE/dx. So we use the proton data set for validation of the detector response at high dE/dx region(See section xxx). We have collected three different Kaon data by varying thickness of the degrader. 540, 630, 680 MeV/c are corresponds to the momentum degraded by 2 lead glass, 1 lead glass + 1 lead block, and 1 lead glass, respectively, and such Kaon stops after 10 cm, 50 cm, and 65 cm of flight distance inside TPC fiducial volume.

Figure 1 shows an 2D display of typical event taken with 800 MeV/c electron trigger. Horizontal axis corresponds to TPC channel number and zero means most upper stream strip. Since strip pitch is 1 cm, this is equivalent to distance from beam injection point in cm. Vertical axis corresponds to electron drift time in μs and t=0 means trigger timing. In this TPC, anode and cathode is located at top and bottom of the detector, respectively, t=0 means energy deposition at anode and longer drift time means energy deposition in lower height. With 200 V/cm of electric field, drift velocity is about 0.8 m/ms. So drift of full detector (40 cm) takes 500 μs. Color strength of the plot corresponds to the TPC signal pulse height in ADC counts which is roughly proportional to dE/dx of the track. In this event, triggered electron can be clearly seen center of the detector as an electromagnetic shower while there are two other particles accidentally overlapped with the triggered electron. Track at t=100 μs is considered as a proton which stops after 15 cm of flight distance and has large dE/dx around the stopped point. Track at t=400 μs is considered as a pion which passes-through the detector and has uniform dE/dx over the TPC channels. This event already gives us some idea for how good the particle identification performance of the LArTPC is.

Figure 2 shows a typical $K \rightarrow \mu\nu$ like event. We can clearly identify a kink of the track at 60 cm which is considered as stopped point of Kaon and it decays to

Energy deposition of the track is about MIP at the injection point and gradually increase towards the stopped point at 60 cm.

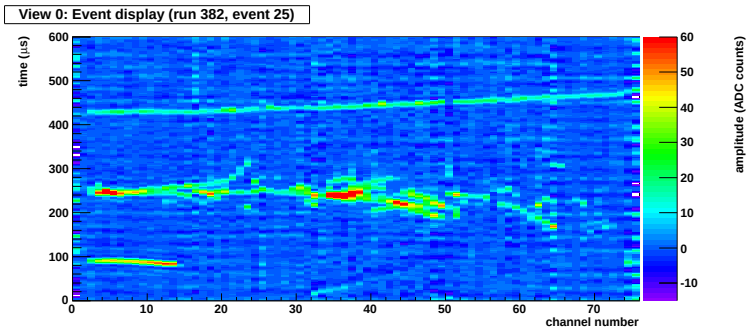

Figure 1: Event display of 800 MeV/c electron triggered event. Accidentally overlapped with a proton and a pion.

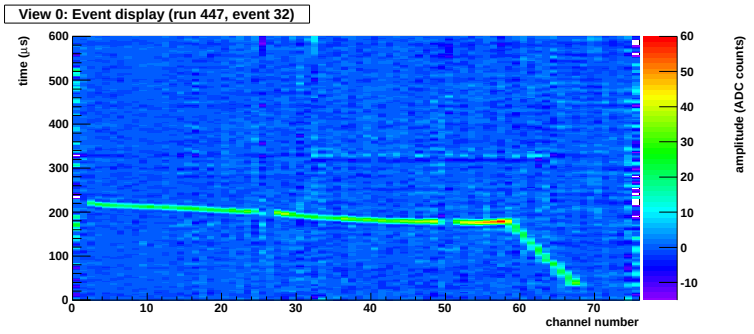

Figure 2: Event display of Kaon 630 MeV/c triggered event

Table 1: List of collected data

Particle	Momentum (MeV/c)	Number of Events
Pion	800	3,000
Proton	800	1,500
Kaon	540 (2LG)	7,000
Kaon	630 (1LG+1LB)	40,000
Kaon	680 (1LB)	35,000
electron	800	2,500
electron	200	10,000
pion	200	10,000

2.2. Beam Quality (Purity)

- Plot: TREK counters (FC, GC, TOF) (A. Okamoto)
- Plot: TOF before and after selection (A. Okamoto)

As described in section xx, we have several beam counters to identify beam particles event by event Figure reffig:TREK shows response of the, FC, GC, and TOF counters. By using these counter information,

Particle	FC(K)	FC(pi)	GC
Pion	x	o	x
Kaon	o	x	x
Proton	o	x	x
electron	x	o	o

Table 2: List of collected data

GC is used to identify electrons

2.3. Beam Energy, Position

3. Beam Energy, Position

3.1. Beam Energy

30GeV proton beam hits to target T1 in Hadron hall. It generates many particles like kaon, pion, muon, electron, and so on. We take the particles that has 800MeV/c momentum from this beam by using D1 magnet.
For this analysis, a beam momentum at BDC after passing through the

K1.1Br beam line is required. We estimate a beam momentum using simple MC simulation. Figure 4 shows MC simulation's geometory. This time, beam line is straight and has no electric and magnetic field. MC simulation shoot 800MeV/c kaon and pion as pencil beam.

Figure 5 shows kaon and pion momentum distribution using this MC simulation. Actually, kaon momentum distribution peak is adjusted so that kaon decay point of MC simulation is consistent with data. Section 3.1.1 explains this point. And proton momentum is estimated in other way, using TREK detector TOF information. Section 3.1.2 shows proton momentum distribution.

3.1.1. Kaon energy

We adjust momentum peak of figure ?? and set Kaon beam energy the point that the decay points of Kaon in data and simulation are good agreement. The distribution of decay poins are plotted in Figure3.

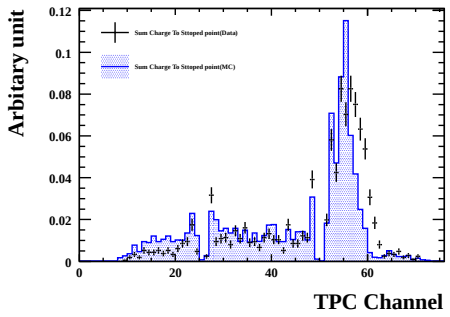

Figure 3: Decay point distribution of Data and MC

3.1.2. Proton energy

asuka

3.2. Energy deposition in degrader

Because of having high energy, kaon beam from BDC passes through 250LAr TPC. So that kaon stops in 250LAr TPC, we put degrader, which reduce beam energy, on beam line. In this experiment, we used lead glass and lead block as degrader. We estimate energy deposition in degrader by using MC simulation. Figure 6 shows energy deposition in degrader.

3.3. Beam Position

Before taking data, we measured a beam profile on the front of 250LAr TPC by using plastic scintillation counter. Figure 7 shows beam profile on the front of 250LAr TPC.

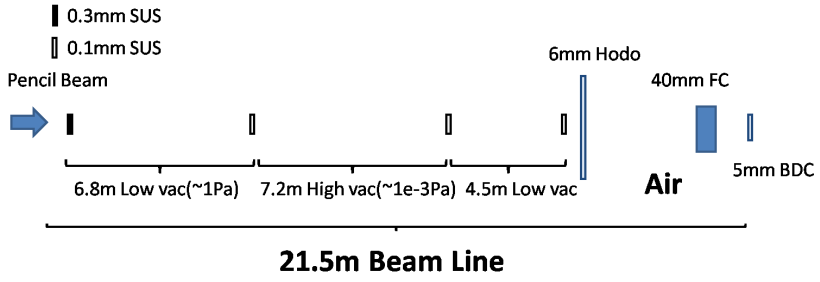

Figure 4: K1.1 Br beamline

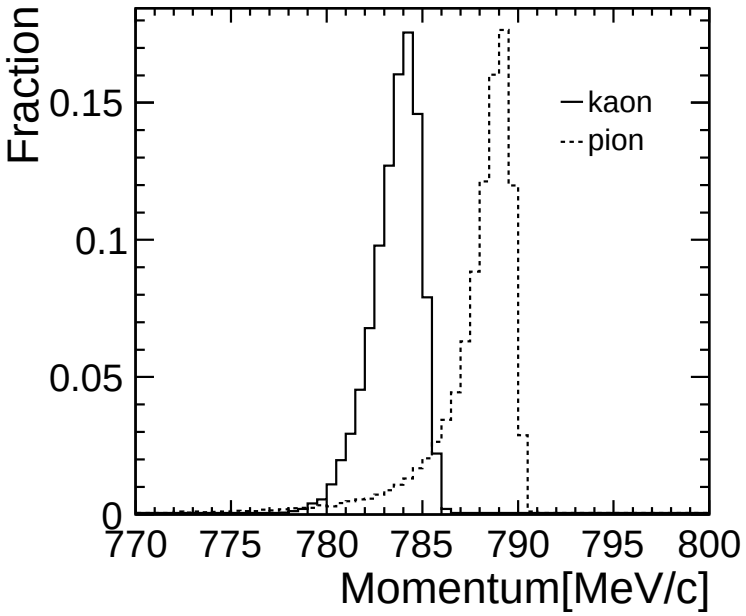

Figure 5: kaon and pion momentum distribution at BDC

- Plot: Proton momentum from TOF (A. Okamoto)

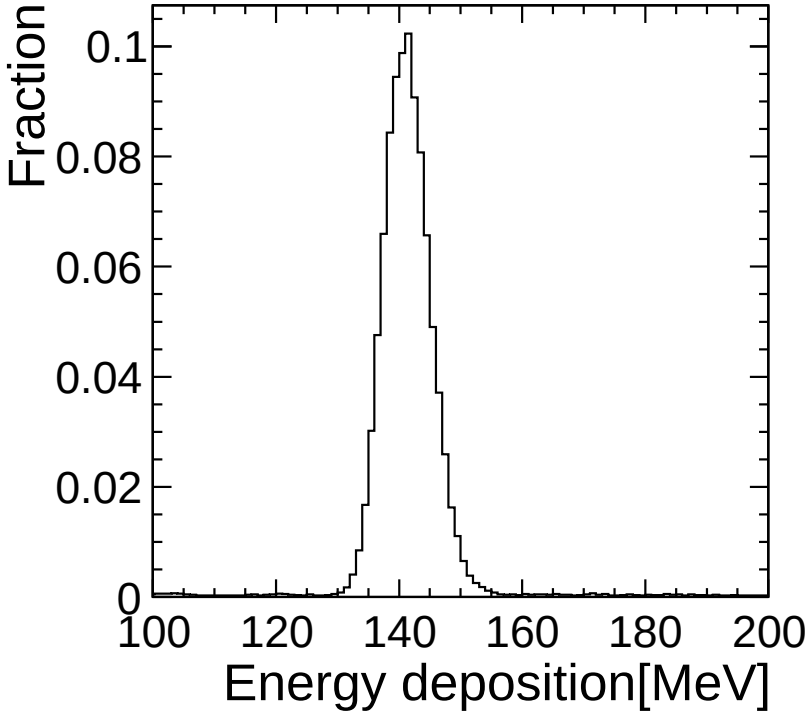

Figure 6: energy deposition in degrader

- Kaon:: Ongoing (H. Okamoto?)
- Plot: Beam position measurement

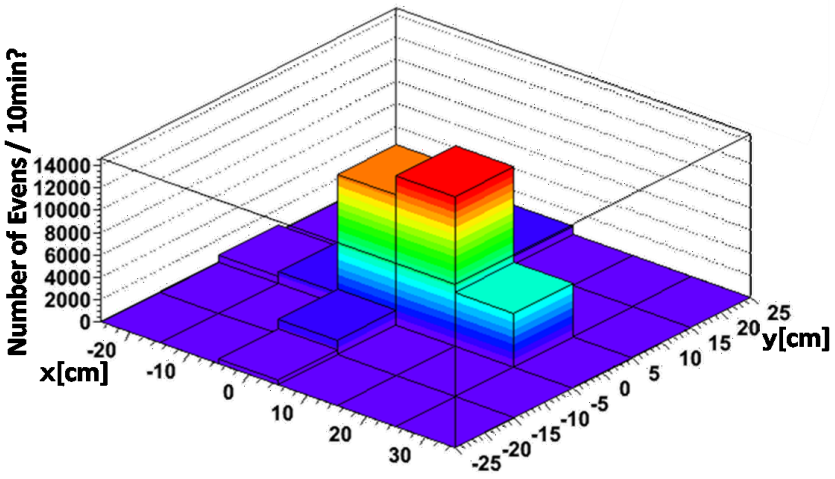

Figure 7: Beam profile on the front of 250LAr TPC

4. Software Framework

For analyzing the data, we have used a

Qscan is a general purpose software package for LArTPC analsys which provides, event reconstruction: noise reruction, hit finding, clustering, and tracking event simulation: GEANT VMC with ROOT geometry, event visualization: raw data and reconstructed data display ....

5. Event Reconstruction

5.1. Noise Reduction

Figure 9 shows raw waveform of the TPC signal before applying any noise reduction. Two waveforms shown in this plot are channel 13 and 37 in Figure 1 which are roughly proton stopped point and electron shower maximum point, respectively. Signal-to-noise ratio for this particular case is poor and pion signal which is supposed to be t=400 μs is almost hidden by the noise. While time width of TPC signal is few μs which is determined by drift time between anode and anode-grid, dominant noise component looks higher frequency. To reduce such noises, we have applied FFT (Fast Flourier Transformation) filter to cut the high frequency component. Figure **??** shows amplitude as a function of frequency for the same event. This clearly shows dominant noise component with $>$ 200 kHz has good separation with signal component ($<$ 100 kHz). Figure 10 shows the waveform after removing high frequency ($>$ 80 kHz) component by the FFT filter. Signal-to-noise ratio is dramatically improved. On the other hand, we expect certain bias to the signal charge measurement by this filter, and it will be discussed in Section x.

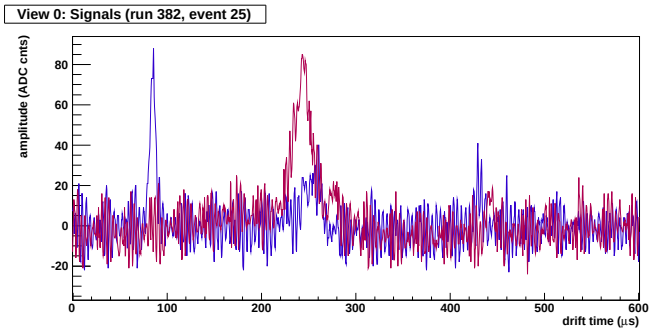

Figure 8: TPC raw signal waveform for "Textbook" event channel 13 and 37.

After noise reduction we find signal hits and create clusters associated to single tracks. Hit is defined as bump over given threshold in a channel. After finding all hits in an event, we construct cluster by merging adjacent hits. The example of hit finding and clustering is shown in Fig 11, which indicates reasonable hit and cluster findings. Threshold of hit finding is six for our analysis. Monte Carlo simulation shows 99.8% and 81.8% hit finding

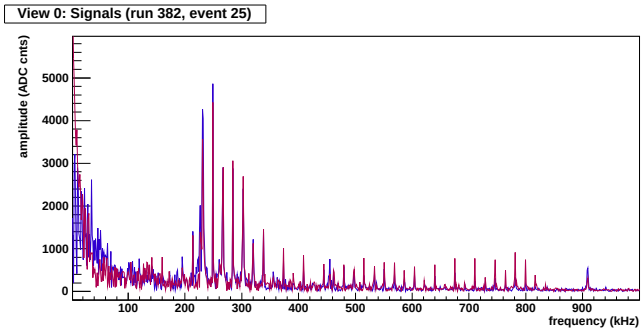

Figure 9: FFT frequency amplitude distribution

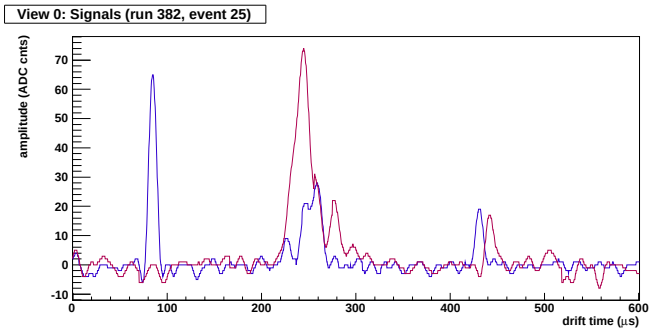

Figure 10: TPC signal waveform after cutting the frequency $>$ 80 kHz.

efficiencies for Kaon and decayed muon hits, respectively. Average noise hits are about 7.5 in an event.

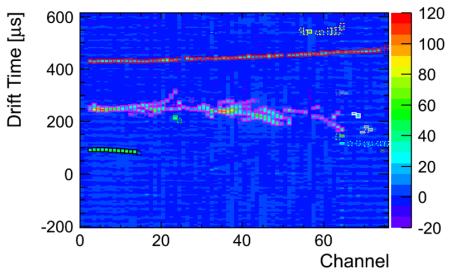

Figure 11: Example of hit finding and clustering. A colored box corresponds to a hit and colors represent different clusters.

- Plot: Finding efficiency vs threshold (Naganoma): TBU
- Plot: Through-going pion data Q vs pion (Tanaka)

5.2. Stopped Point Finding

5.2.1. Proton

5.3. Stopped Kaon

Hough transform was invented for machine analysis of bubble chamber photographs by Paul.V.C.Hough.[6] We detect straight lines using hough method , and find Kaon stopped point from the intersection of straight lines. Figure 12 shows hit map like a Kaon track. One point in the X-Y space can be transformed into sinusoidal curve in the ρ-θ space.Figure 13 shows sinusoidal curves in all points. And, we detect the straight line associated with the largest number of points by choosing the most dense point in ρ-θ space. Next , the sinusoidal curves of the hits associated with frist straight line are removed from figure 13. Figure 14 shows sinusoidal curves after the hits associated with frist straight line removed. We detect second straight line using the same procedure.This procedure is repeated until there are less than three points.Figure 15 shows the two straight lines detected by hough transform mehotd.
Kaon stopped point in the liquid argon detecor defined as charge maximum point around the intersection of some lines.

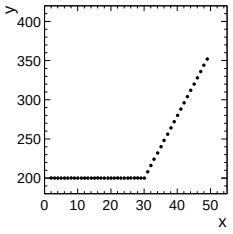

Figure 12: Hit map like a Kaon track

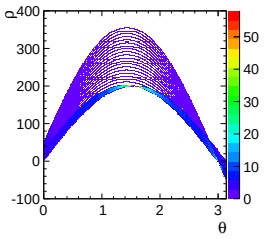

Figure 13: sinusoidal curves getting form all hough transformed points of Figure 12

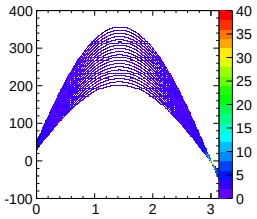

Figure 14: sinusoidal curves removed the points associated with first straight line from figure 13

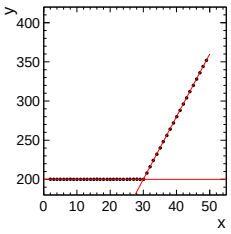

Figure 15: Two lines detected with hough transform method

5.3.1. Chi2 method

χ^2 method is the algorithm that search the point of rapidly increasing fit'χ^2 and the point defined as the stopped point. Because the charged particle coming from upsteam of beam line , track reconstruction is started from minimum channel to the maximum channel of the cluster.
Figure 16 shows hit map like a Kaon track. We start fitting with straight line from minimum channel to maximum channel.Figure 17 shows range vs fit'χ^2 distribution. As it can be noiced for figure 17, χ^2 is increased rapidly if the straight line is strayed out. Then , we search the strayed point from the straight line by setting reasonable threhold and draw from minimum channel to the strayed point. This procedure is done from maximum channel to minimum channel in the same way. And we draw from maximum channel to the strayed point. Kaon stopped point in the liquid argon detecor defined as charge maximum point around the intersection of two lines.

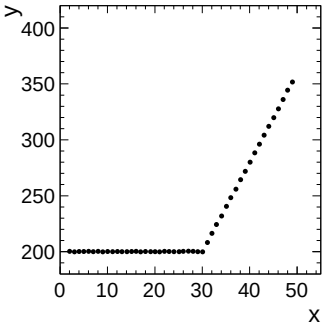

Figure 16: hit map like a Kaon track

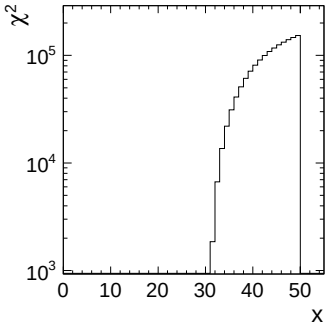

Figure 17: range vs χ^2 distribution

5.3.2. BS method

In the χ^2 method , we can't detect Kaon stopped point in the case of backward decay. Then , we detect Kaon stopped point using BS method.
BS method is concept that the Kaon stopped point defined as lightmost channel in the case of backward decay. we descript below how the track defined as backward decay. N_1 is defined as Number of cluster hits found by the clustering. Stopped point finding is started from minimum channel. We search for the closet timing hit in next channel from current channel hit. Then , we repeat this procedure until maximum channel and count the number of selected hit information(N_2). In the case of backward decay , N_1 is larger than $N2$. So , we set reasonable threhold of the difference between N_1 and $N2$, and if the $N_1 > N_2$ is over the threshold , the track is defined as backward decay. In the case of backward decay , we defined charge maximum point around the maximum channel as the stopped point.

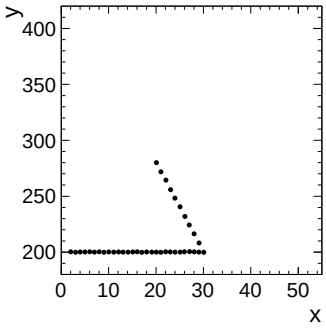

Figure 18: hit map like a Kaon track

6. Liquid Argon Purity

Attenuation of the drift electron depends on purity of LAr since electronegative impurities capture it [5]. Thus we need to apply correction to TPC signal charge depends on the drift time. We use cosmic ray sample triggered by inner PMT at off-beam timing for measuring the LAr purity, and use this to correct the beam data. Figure 19 shows an event display of typical cosmic muon event across TPC channels. The attenuation of readout charge depending on drift time is clearly seen in the right plot. Readout charge in an event cannot be fitted by exponential because energy deposition follows Landau distribution and charge readout is affected by electric field distortion which is described latter in section **??**.

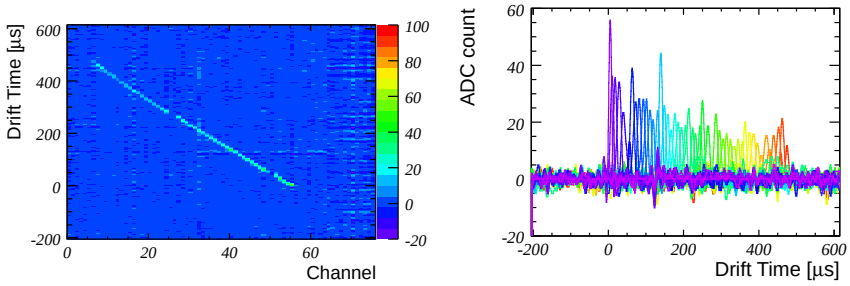

Figure 19: Left: Typical cosmic muon event across TPC channels. Right: Charge deposit as a function of drift time. Colors correspond to different TPC channels.

We select cosmic ray event with more than 20 TPC channels which corresponds to zenith angle of more than 27° and consistent with straight line by χ^2 fit. Readout charge is corrected for field distortion and projected to beam direction to correct injection angle. We fit readout charge by Landau function in each drift time bin to estimate average charge deposit. Figure 20 shows example of the average readout charge as a function of drift time is fitted by exponential to obtain drift electron lifetime. Realistic Monte Carlo simulation shows about 13% (TBU) smaller lifetime estimation due to noise, field distortion, and FFT effects. We correct output lifetime from these effects. Figure 21 shows an drift electron lifetime as a function of duration after initial LAr filling. Drift electron lifetime was 600 μs at 60 hours, and 400 μs after 150 hours. The degradation is possibly due to impurity from micro

leak or out-gassing penetrating faster than purification by gas recirculation. But we kept enough drift electron lifetime during data taking period.

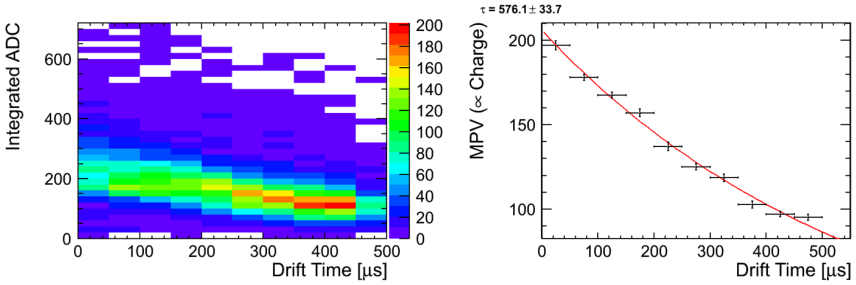

Figure 20: TBU. Left: Readout charge as a function of drift time. Readout charge in each drift time bin is fitted by landau function. Right: Average charge readout as a function of drift time which is fitted by exponential to estimate drift electron lifetime.

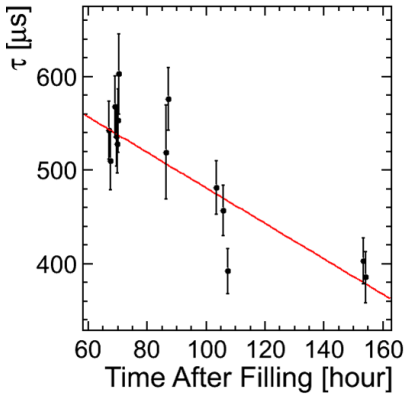

Figure 21: TBU. Drift electron lifetime as a function of duration after initial LAr filling. The lifetime is used to correct the beam data.

7. Event Simulation

7.1. Geant3, recombination, drift velocity

We use GEANT3 for simulating energy deposition of beam particles and their daughters. Readout pitch is 1 cm,

we set the maximum step of Geant to 0.5 mm which is enough smaller than the readout pitch of 1 cm.

It means charge deposition in one strip is typically simulated with 20 GEANT steps.

We set energy cut-off for soft electron/photon emission to 10 keV which is minimum possible energy can be set in GEANT3. This cut-off is very important for ionization electron recombination.

Recombination of electron and Argon ion depends on the electric field and dE/dx. We use a measurement in Ref.[3].

$$Q = A\frac{Q_0}{1 + kdE/dx}, A = 0.800, k = 0.486 \quad (1)$$

Velocity of the drift electron depends on the liquid Argon temperature and the electric field. We use a measurement in Ref [4].

```
*     Special TPAR for TMED   3   Liquid_argon
*  CUTGAM= 10.00 keV  CUTELE= 10.00 keV  CUTNEU= 10.00 MeV  CUTHAD= 10.00 MeV
*  BCUTE = 10.00 keV  BCUTM = 10.00 keV  DCUTE = 10.00 keV  DCUTM = 10.00 keV
*  IPAIR=  1.  ICOMP=  1.  IPHOT=  1.  IPFIS=  0.  IDRAY=  1.  IANNI=  1.  IBR
*  IMUNU=  1.  IDCAY=  1.  ILOSS=  1.  IMULS=  1.  IRAYL=  0.  ILABS=  0.  ISY
```

- Plot: Geant Geometry, typical track (Tanaka)
- Plot: recombination factor, drift velocity (Tanaka)

7.2. Electric Field

Electric field of the TPC field cage We have calculated the electric field using a 2D FEM (Finite Element Method) package [**?**].

This field map is used for simulating electron drift.

- Plot: 2D field map (Tanaka)

7.3. Drift Electron Diffusion

- Plot: drift simulation (Tanaka)

7.4. Preamp Gain Calibration

- Preamp gain vs channel number (Naito)

7.5. FFT Noise

Adding realistic noise to MC simulation is very important. In this section, we will introduce how to make realistic noise and implement to MC.

7.5.1. Noise information of Real DATA

As a first step, we checked distributon of frequency from real data using FFT(Fast Fourier Transform)(see Fig22). Next, We got distribution of amplitude value channel by channel and frequency by frequency. Fig22 shows an example. In this event, amplitude is 200 about 400 [kHz] in 10 channel. After repeating this procedure, we could obtain histograms of amplitude value channel by channel, frequency by frequency(23). We used these histograms to reproduce realisitic noise. Details are described in the next section

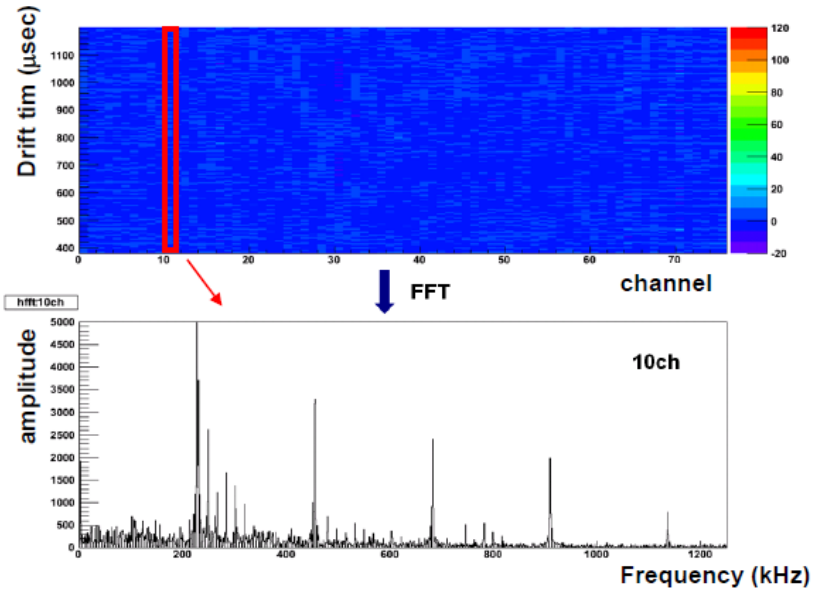

Figure 22: example distribution of frequency:10ch

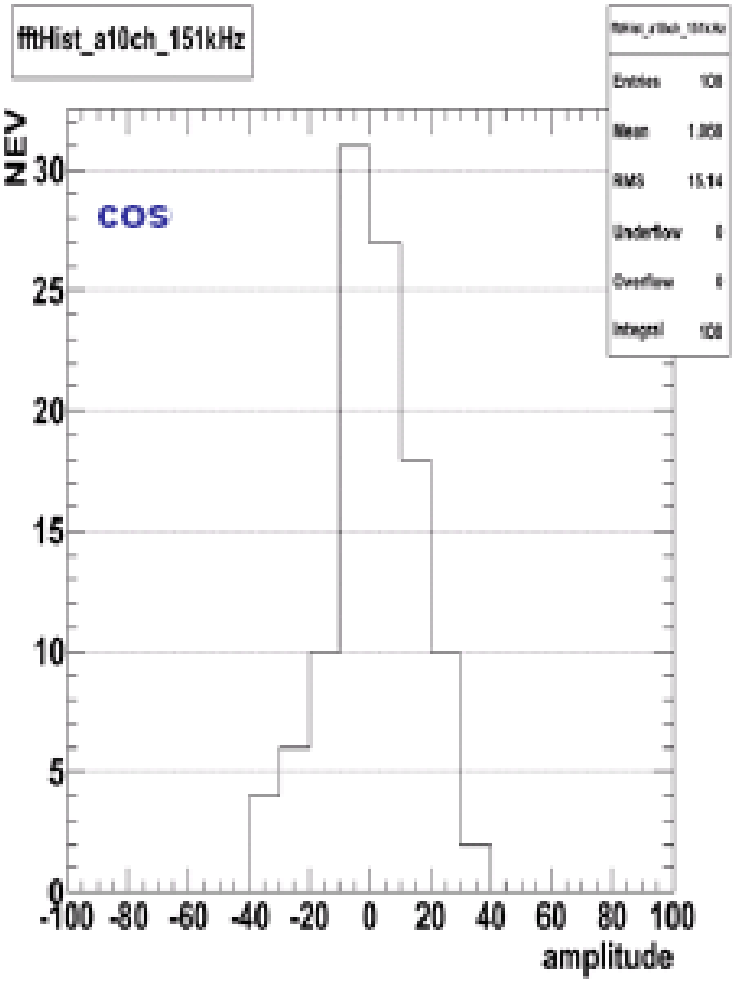

Figure 23: An example of distribution of amplitude

7.5.2. Making FFT noise

The procedure of making FFT noise is below:

1. Get amplitude from the histograms of amplitude at random.
2. Perform Inverse FFT

After performing inverse FFT, there is random noise (Fig24)which have the same distribution of frequency as real data. Real DATA have coherent noise

but random noise don't have coherent components, therefore adding coherent components is necessary to reproduce realistic noise.

3. Select random noise 0 and 31 and 63ch
4. Insert random noise 0 ch to 1-30ch, 31ch to 32-62ch, 63ch to 64-75ch
5. Scaling each channel

Real DATA look having coherent noise board by board(We used 3 readout board in T32 experiment). We chosen 3 random noise(0ch,31ch,63ch) in this reason. After that, each channel needs to be corrected as each noise scale. Fig25 shows coherent noise after scaling as Fig26. Vertical axis of Fig26 is RMS of FADC, it stands for noise level.

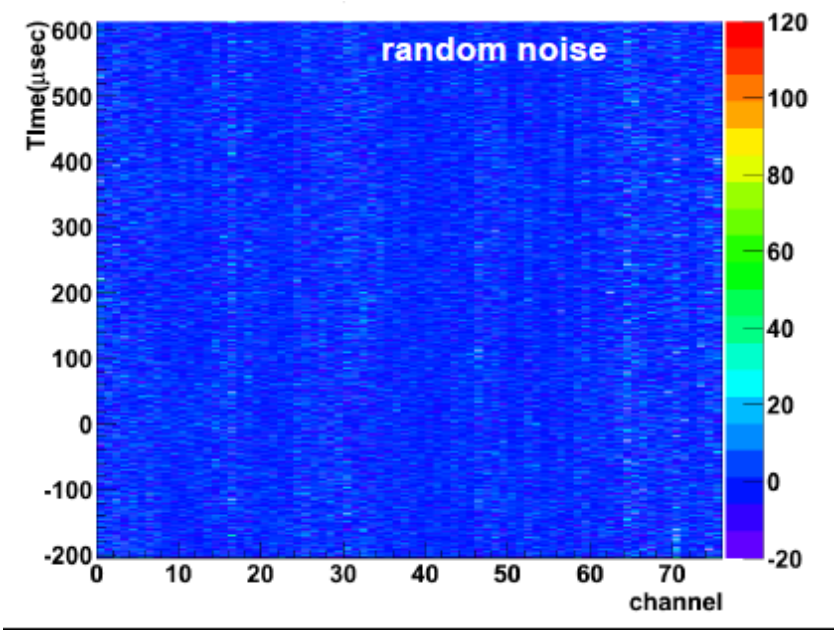

Figure 24: Random noise

6.Mixing Random noise and Coherent noise.

Finaly, We mixed Random noise and coherent noise as

$$RealisiticNoise = RandomNoise + CoherentNoise * 0.5 \qquad (2)$$

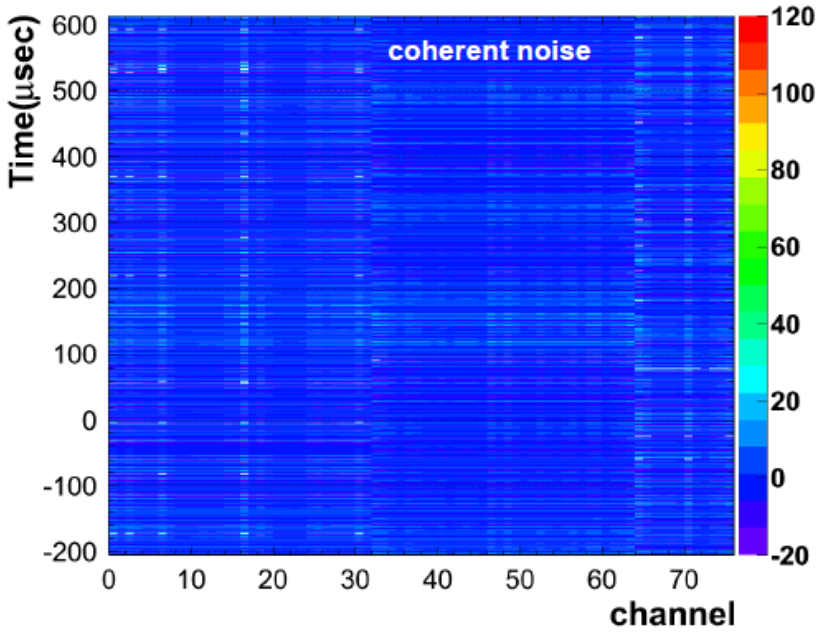

Figure 25: Coherent noise

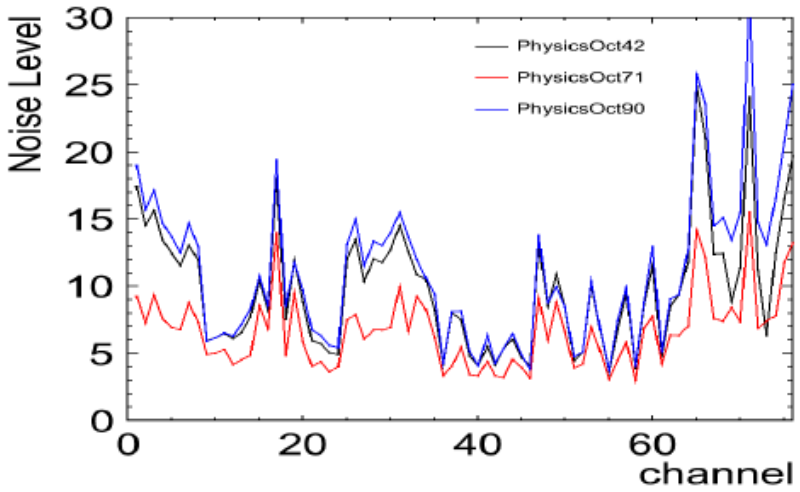

Figure 26: Noise level

- Plot: simulated event (Nagasaka)

7.6. Cross Talk

- Plot: signal waveform (proton stopped point + 1) (A. Okamoto)
- Plot: simulated event with and without cross talk (A. Okamoto)

7.7. Signal and Noise Scale Tuning

- Plot: Landau distribution after the tuning (Tanaka)

8. Data- MC Comparison

8.1. Through-going Pion

- Plot: Data-MC comparison (Tanaka)

8.2. Stopped Proton

- Plot: Hit charge, cluster charge, stopped point (A. Okamoto)
- Plot: hit charge with different distance from SP (A. Okamoto)
- Plot: average hit charge vs different distance from SP (A. Okamoto)

8.3. Recombination Factor

Electron-ion recombination depends on the electric field and stopping power dE/dx. We have studied this factor using tagged proton beam. Recombination factor measurement using proton beam is relatively easy because of stability of proton. This is why we used proton beam for this study as a first step.
Expression for recombination can be derived

$$Q = A\frac{Q_0}{1 + (k/E) \times (dE/dx) \times (1/\rho)} \tag{3}$$

where Q_0 is initial ionization charge, E is electric field, dE/dx is energy deposit per distance, ρ is density of liquid Argon, A and k are fit parameters. This formula can be rearranged like below:

$$\frac{Q_0}{Q} = \frac{1}{A} + \frac{(k/E)(dE/dx)(1/\rho)}{A} \tag{4}$$

The ratio of Q_0/Q depends on stopping power dE/dx, so we determined fit parameter A and k using proton data and Monte Carlo simulation. In this analysis, we need Q, Q_0 and dE/dx channel by channel. First, Electric Field E is fixed at 0.196 [kV/cm]. Second, Q is integrated charge in an anode readout channel. we can get this value from Real DATA. Third, Q_0 is integrated charge without recombination factor in an anode readout channel. This value can be obtained using Qscan. And then, dE/dx per an anode channel is determined with truth information of Qscan MC. Fig27, 28, 29 shows Q, Q_0, $dEdx$ from stopped channel -1 to stopped channel -14. In many case, integrated charge in stopped channel are composed of cross talk. This is the reason why we don't use information from stopped channel in this analysis.

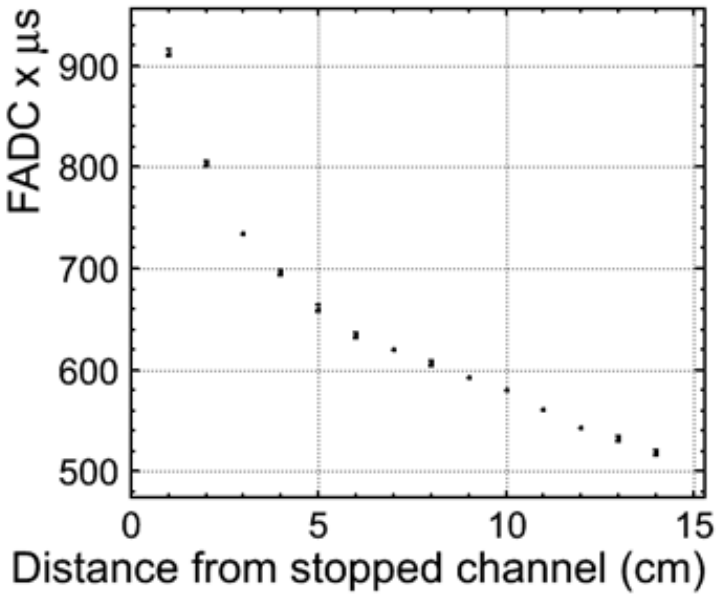

Figure 27: DATA:Integrated Flash ADC counts from stopped channel -1

The result of this study is shown in Fig30. Vertical axis is Q_0/Q, and horizontal axis is dE/dx in this figure, this plot is fitted by Birk's low. As a result, we got fitting parameter

$$\begin{aligned} A = & \quad 0.782 \pm 0.009 \\ k = & \quad 0.0467 \pm 0.0009 [kV(g/cm^2)/cm/MeV] \end{aligned} \tag{5}$$

We checked Birk's low in the range 4 $[MeV/(g/cm^2)] \leqq dE/dx \leqq 12$ $[MeV/cm^2]$ and the result is consistent with ICARUS experiment's one in – sigma.

8.4. Stopped Kaon

In this section , we compare some quantities of data and MC simulation that K stop in the liquid argon detector and can detect stopped point. Figure 31-34 shows Data and MC comprison for signal hit charge , sigmal width , cluster charge and primary paricle charge distribution. Data of signal charge and signal width are consistnt with MC one in error by less than two % and

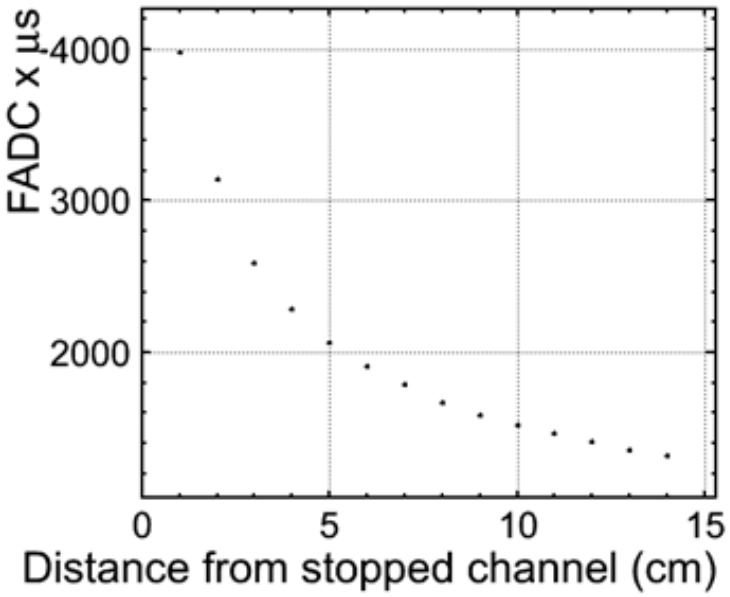

Figure 28: MC without recombination:Integrated Flash ADC counts from stopped channel -1

data of cluster charge and parimary charge are consistent with MC one in error by less than five %.

Figure 8.4 shows signal hit charge distribution of restricted channel 27. As it can be noiced for figure 8.4 , signal charge have two peaks at 300 and 500 dQ/dx. Because two peaks has correlation of ΔTOF , there is some possibility of not passig in the center of the detector. So , we use only the event that signal charge of restricted channel 27 is less than 350. Figure 36 shows signal hit charge distribution in different distance from the stopped point.

As it can be noticed for figure 36 , data plot is consistent with MC one. Figure 37 shows data/MC ratio of signal hit charge distribution in different distance from the stopped point. Data of signal charge in dirfferent distance from stoppd point are consistnt with MC one in error by less than five %

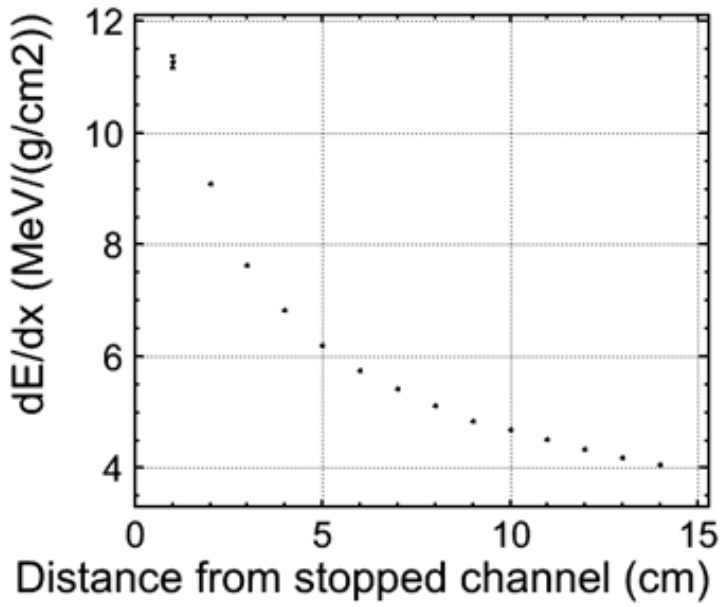

Figure 29: dE/dx from stopped channel -1

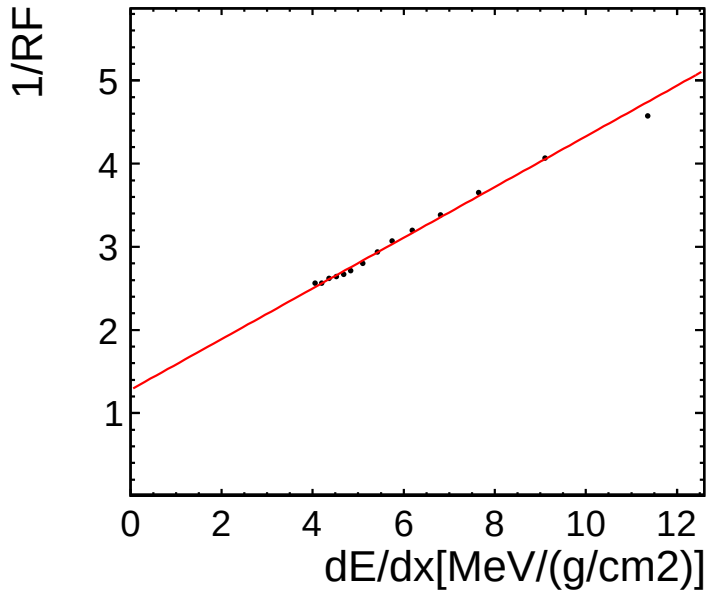

Figure 30: 1/RF VS dE/dx: fitted by Birk's low

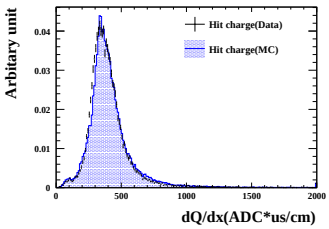

Figure 31: Data-MC comparison for hit charge in all range

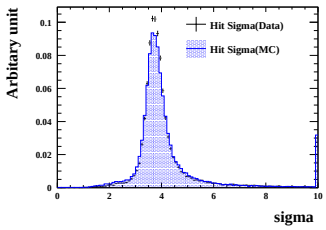

Figure 32: Data-MC comparison for hit sigma in all range

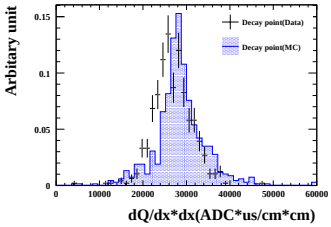

Figure 33: Data-MC comparison for Cluster Charge

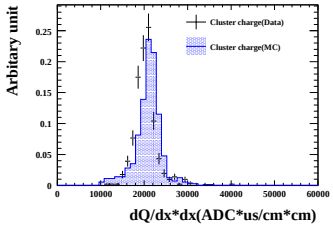

Figure 34: Data-MC comparison for Primary particle charge

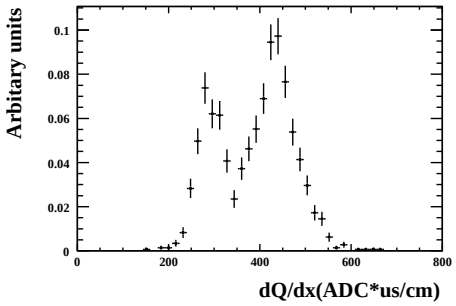

Figure 35: Hit charge in channel 27

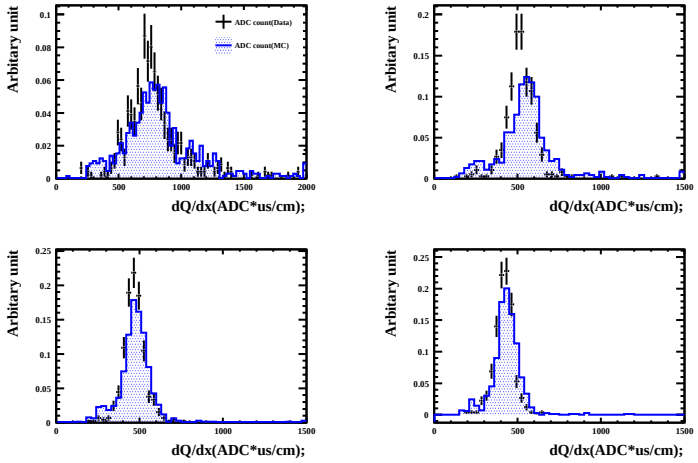

Figure 36: Data-MC comparison for hit charge distribution in different distance from the stopped point(top left:decay point,top light:decay point-5cm,bottom left:decay point-10cm,decay point-15cm)

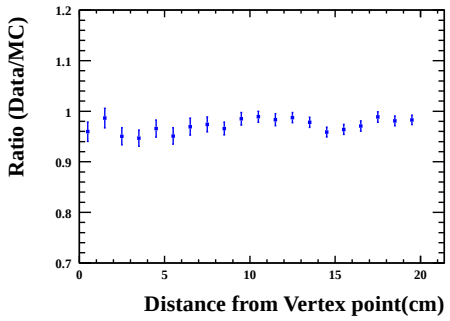

Figure 37: Data/MC ratio for hit charge distribution in different distance from the stopped point

9. Summary

References

[1] O. Araoka *et al.*, J. Phys. Conf. Ser. **308**, 012008 (2011) [arXiv:1105.5818 [physics.ins-det]].

[2] S. Mihara [MEG Collaboration], Nucl. Instrum. Meth. A **518**, 45 (2004).

[3] S. Amoruso *et al.* [ICARUS Collaboration], Nucl. Instrum. Meth. A **523**, 275 (2004).

[4] S. Amoruso, M. Antonello, P. Aprili, F. Arneodo, A. Badertscher, B. Baibusinov, M. Baldo-Ceolin and G. Battistoni *et al.*, Nucl. Instrum. Meth. A **516**, 68 (2004).

[5] A. Bettini *et al.*, Nucl. Instrum. Meth. A **305**, 1991 (177).

[6] P.V.C Hough 'Method and means for recognizing complex patterns',United States Patent Office 3069654(1962)